

# Broadband mid-infrared frequency upconversion and spectroscopy with an aperiodically poled LiNbO<sub>3</sub> waveguide

Tyler W. Neely,<sup>1,2,†</sup> Lora Nugent-Glandorf,<sup>1,†</sup> Florian Adler,<sup>1</sup> and Scott A. Diddams<sup>1,3</sup>

<sup>1</sup>National Institute of Standards and Technology, Time and Frequency Division, Mail Stop 847, 325 Broadway, Boulder, Colorado 80305, USA

<sup>2</sup>e-mail: t.neely@uq.edu.au

<sup>3</sup>e-mail: scott.diddams@nist.gov

Received July 10, 2012; accepted September 9, 2012;

posted September 13, 2012 (Doc. ID 172303); published October 12, 2012

We convert a mid-infrared frequency comb to near-infrared wavelengths through sum-frequency generation with a 1.064  $\mu\text{m}$  CW laser in an aperiodically poled ZnO:LiNbO<sub>3</sub> waveguide. Upconversion of light in the range of 2.5–4.5  $\mu\text{m}$  to 0.76–0.86  $\mu\text{m}$  is demonstrated in a single device, and the efficiency of the conversion is measured across this bandwidth. We additionally characterize the spatial mode of the upconverted light. We then use this upconversion technique to detect and resolve individual lines from a methane gas sample with a common near-infrared optical spectrum analyzer. The stability of the spectrum of the upconverted light is analyzed with the goal of evaluating this technique for precise spectroscopic measurements. © 2012 Optical Society of America

OCIS codes: 190.7220, 140.7090.

Mid-infrared (MIR) frequency comb sources have seen increasing application in the fields of metrology and molecular spectroscopy due to their broad bandwidth, access to diverse wavelengths, high spectral brightness, and narrow comb-tooth linewidth [1–6]. Most approaches have relied on single point detection techniques such as multiheterodyne detection [1,6] and Fourier transform interferometry [2]. Recently, however, we have demonstrated direct detection with a two-dimensional-array MIR virtually imaged phased-array spectrometer [7]. Nonetheless, when compared with the near infrared (NIR), working directly in the MIR has drawbacks due to more specialized optics and components along with less sensitive, more expensive, and lower bandwidth detectors. A demonstrated technique to circumvent these challenges is to implement detection in the NIR through upconversion of the MIR light through sum-frequency generation (SFG) [5,8–10]. This enables the usage of standard Si-based detectors and more readily available optics and spectrometers.

In our previous work we employed bulk sum-frequency crystals that limited the conversion bandwidth and efficiency [5]. Here, we demonstrate broadband up-conversion of light spanning 2.5 to 4.5  $\mu\text{m}$  through SFG with CW 1064 nm light, by use of a linearly chirped aperiodically poled ZnO:LiNbO<sub>3</sub> (aPPLN) waveguide [11–14]. Additionally, by confining both the 1064 nm pump and MIR waves along the length of the waveguide, a significant increase in conversion efficiency is seen when compared with a bulk PPLN upconversion crystal. For frequency comb spectroscopy this improved efficiency is important because CW light must be used to maintain a unique mapping between MIR and NIR comb teeth.

Figure 1 outlines the experimental setup. The output of a 100 MHz femtosecond Yb-fiber oscillator [15] is amplified using a double-clad Yb: fiber amplifier, producing output pulses centered at 1060 nm, with average power of up to 6 W, and 170 fs duration after recompression. These amplified pulses pump a singly resonant optical

parametric oscillator (OPO) based on a fan-out, periodically poled, MgO:LiNbO<sub>3</sub> (PPLN) crystal [16]. By translating the fan-out PPLN crystal, the MIR idler spectrum is tunable from 2.5 to 4.5  $\mu\text{m}$ , with up to 500 mW average power, and greater than 200 nm FWHM bandwidth at a single tuning point.

The MIR pulses are combined with 350 mW of 1064 nm CW light from a Nd:YAG laser, and both wavelengths are coupled into a custom-designed 16.4  $\mu\text{m}$   $\times$  10.1  $\mu\text{m}$   $\times$  40 mm aPPLN waveguide [14]. The poling period of the aPPLN is chirped linearly across the length of the waveguide from 18.8 to 21.8  $\mu\text{m}$ , providing phase matching across the tuning range of the MIR source and upconverting the light to NIR wavelengths. The input face of the aPPLN is anti-reflection (AR) coated for 1064 nm and 2.5 to 4.5  $\mu\text{m}$ , while the output is AR coated for 750 to 900 nm. The average coupling efficiency of the pump wavelength through the waveguide is 74%. On average the MIR coupling is measured to be 33%; however, we take this value as a lower bound, as the effect of the output AR coating on the MIR wavelengths is not specified.

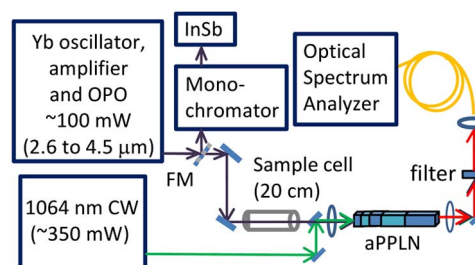


Fig. 1. (Color online) Amplified Yb: fiber OPO laser system is used to generate tunable MIR light tunable from 2.5 to 4.5  $\mu\text{m}$ . The MIR light is combined with a CW 1064 nm Nd:YAG laser in an aperiodically poled LiNbO<sub>3</sub> waveguide (aPPLN). After a short-pass filter, the upconverted light is coupled into a single-mode fiber and sent to an optical spectrum analyzer (OSA). The MIR spectrum is recorded using a monochromator and InSb photodiode via insertion of a flip mirror (FM) in the beam path.

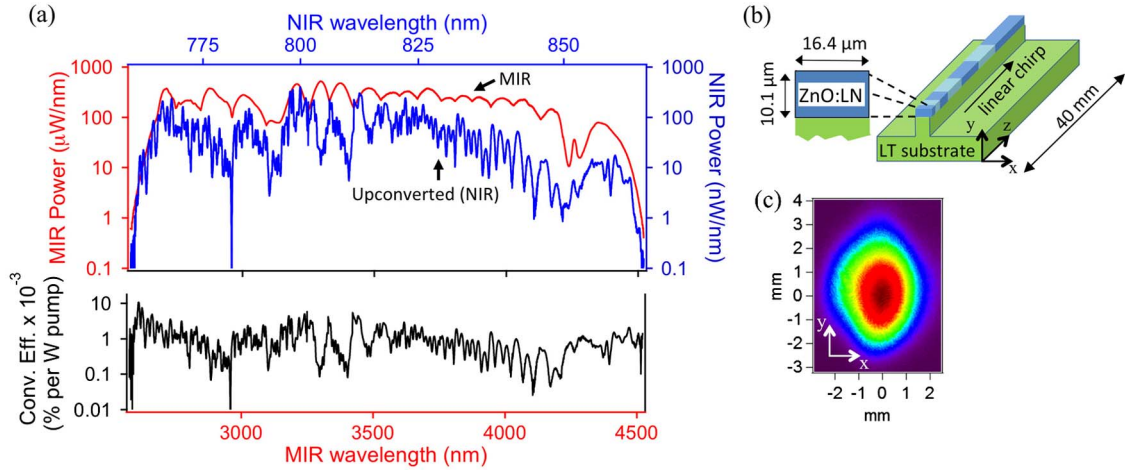


Fig. 2. (Color online) Broadband MIR light upconverted in a waveguide aPPLN. (a) Concatenated OPO spectrum (red top curve), and corresponding sum frequency spectrum (blue middle curve) converted to MIR wavelengths. Calculated conversion efficiency (black) of the waveguide aPPLN, relative to the coupled pump power. (b) Schematic of the upconversion waveguide chip. The waveguide consists of ZnO-doped LiNbO<sub>3</sub> on a lithium-tantalate (LT) substrate, with linearly chirped poling periods (chirp exaggerated for clarity). (c) Output collimated upconverted mode profile.

The resulting broadband upconversion is shown in Fig. 2(a), where MIR wavelengths spanning a range greater than 2000 nm are upconverted. Both MIR and upconverted spectra were measured across the tuning range of the OPO, and then concatenated to allow investigation of the bandwidth of the upconversion process. The oscillatory structures seen in the upconversion efficiency are a result of the wavelength-dependent phase-matching condition across the aperiodically poled waveguide; the poling period is not apodized. An image of the sum-frequency beam, exiting the aPPLN, is shown in Fig. 2(c).  $M^2$  values of 1 and 1.9 were measured for the horizontal and vertical beam dimensions, respectively, and 25% of this light could be coupled into the single-mode fiber.

The conversion efficiency is shown in Fig. 2(a) in units of  $\%W^{-1}$  relative to the pump power. As an example, the average power across the MIR peak at 3630 nm was 143 mW, measured at the input to the aPPLN, and 21.4  $\mu\text{W}$  in the upconverted spectrum, resulting in an efficiency of  $5.8 \times 10^{-2} \%W^{-1}$ , integrated across the upconverted spectrum. This efficiency represents a more than  $\sim 30\times$  improvement when compared to our previous measurements with a bulk PPLN crystal [5].

To demonstrate the potential for spectroscopy, we fill the 20 cm sample cell, shown in Fig. 1, with 2 Torr of pure methane. Both a signal spectrum with the methane sample and a background spectrum with an evacuated cell were acquired with a standard optical spectrum analyzer (OSA). An absorption lineout resulting from the division of background and signal spectra is shown in Fig. 3(b), and compared with the upconverted line centers from the HITRAN database. We note that although the line centers are determined, issues with the peak heights are apparent, with some peaks dropping below zero. These artifacts correspond with both poor signal-to-noise in the upconverted spectrum as well as peak locations on the edges to the upconverted spectral variations. An aPPLN crystal that is properly apodized may alleviate this problem by smoothing the phase-matching response of the crystal [17]; such techniques have been used with success for parametric amplification over a similar

phase-matching range [18]. Nonetheless, we note the novelty of resolving MIR spectral features by use of a relatively nonspecialized NIR OSA.

Stability of the upconverted spectrum is important for applications where accurate knowledge of weak absorption features requires background subtractions and multiple spectral averages. We thus stabilize the OPO at a center wavelength of  $\sim 3.15 \mu\text{m}$  [16] and then record multiple spectra with the OSA, separated by  $\sim 3.44$  s intervals. Absorbance residuals are characterized by the RMS of  $\ln(s_A/s_B)$ , where  $s_A$  and  $s_B$  represent subsequent individual or averaged spectra.

Figure 4(a) shows two upconverted spectra taken 3.44 s apart with an OSA resolution of  $\sim 0.2$  nm, covering a spectral window of 790 to 802 nm. Additionally, a spectrum containing only points exceeding a 5% threshold of the peak value over the spectral window was analyzed to avoid areas of poor signal-to-noise. Examining the results of averaging  $N$  spectra, as shown in Fig. 4(c), the

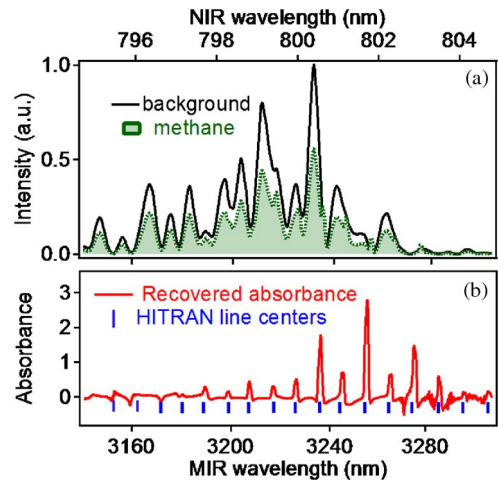


Fig. 3. (Color online) (a) NIR background spectrum (solid curve) and NIR spectrum with methane in the cell (dashed) measured using the OSA (2 s sweep time, 0.05 nm resolution). (b) Recovered methane spectrum with HITRAN line-center comparison.

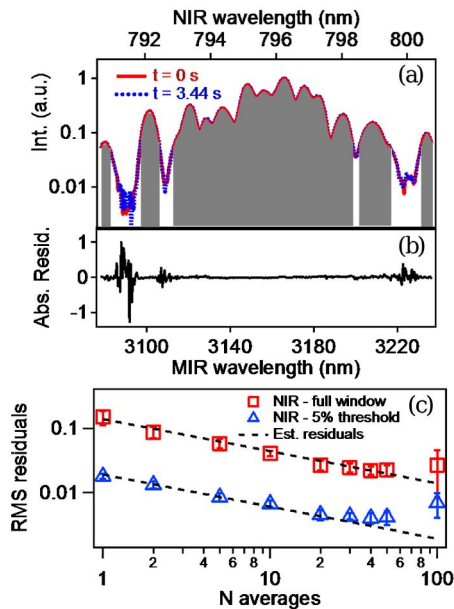


Fig. 4. (Color online) Stability measurements, for a single OPO tuning point. (a) (red, blue-dashed) Two consecutive upconverted spectra showing a repeatable structure, and (gray fill) the spectrum including only points above 5% of the peak value. As seen in the Figure, these spectra are virtually indistinguishable. (b) Absorbance residuals resulting from the division of the red and blue subsequent spectra in (a). (c) Effect of averaging on both the upconverted spectrum over the full window (red squares), data with the 5% threshold (blue triangles). The dashed lines represent fits to a  $N^{-1/2}$  dependence.

behavior closely matches an  $N^{-1/2}$  dependence. However, clear limitations on the absorbance residuals are produced by areas with poor signal-to-noise, as evidenced by the reduced residuals in the 5% threshold data. In this case, a residual level of 0.005 is achieved after 20 averages, or  $\sim 70$  s of data collection. Residual levels on the order of 0.01 are consistent with previous upconversion results utilizing bulk PPLN [5]. With an improved crystal design, such techniques may prove powerful in easing the detection requirements for MIR spectroscopic experiments.

This work was funded by the National Institute of Standards and Technology (NIST) and the United States

Department of Homeland Security's Science and Technology Directorate. It is a contribution of an agency of the U.S. government, and is not subject to copyright in the United States. The authors thank Yoshiki Nishida and NTT Electronics Corporation for fabrication of the aPPLN, and also thank E. Baumann and G. Ycas for their helpful comments. Any mention of commercial products does not constitute an endorsement by NIST.

†These authors contributed equally to this work.

## References

1. F. Keilmann, C. Gohle, and R. Holzwarth, *Opt. Lett.* **29**, 1542 (2004).
2. F. Adler, P. Maślowski, A. Foltynowicz, K. C. Cossel, T. C. Briles, I. Hartl, and J. Ye, *Opt. Express* **18**, 21861 (2010).
3. F. Adler, M. J. Thorpe, K. C. Cossel, and J. Ye, *Ann. Rev. Anal. Chem.* **3**, 175 (2010).
4. B. Bernhardt, E. Sorokin, P. Jacquet, R. Thon, T. Becker, I. Sorokina, N. Picqué, and T. Hänsch, *App. Phys. B* **100**, 3 (2010).
5. T. Johnson and S. Diddams, *Appl. Phys. B* **107**, 31 (2012).
6. E. Baumann, F. R. Giorgetta, W. C. Swann, A. M. Zolot, I. Coddington, and N. R. Newbury, *Phys. Rev. A* **84**, 062513 (2011).
7. L. N. Glandorf, T. Neely, F. Adler, A. J. Fleisher, K. C. Cossel, B. Bjork, T. Dinneen, J. Ye, and S. A. Diddams, *Opt. Lett.* **37**, 3285 (2012).
8. E. J. Heilwell, *Opt. Lett.* **14**, 551 (1989).
9. K. J. Kubarych, M. Joffre, A. Moore, N. Belabas, and D. M. Jonas, *Opt. Lett.* **30**, 1228 (2005).
10. C. R. Baiz and K. J. Kubarych, *Opt. Lett.* **36**, 187 (2011).
11. G. Imeshev, M. A. Arbore, M. M. Fejer, A. Galvanauskas, M. Fermann, and D. Harter, *J. Opt. Soc. Am. B* **17**, 304 (2000).
12. H. Suchowski, D. Oron, A. Arie, and Y. Silberberg, *Phys. Rev. A* **78**, 063821 (2008).
13. H. Suchowski, V. Prabhudesai, D. Oron, A. Arie, and Y. Silberberg, *Opt. Express* **17**, 12731 (2009).
14. Y. Nishida, H. Miyazawa, M. Asobe, O. Tadanaga, and H. Suzuki, *Electron. Lett.* **39**, 609 (2003).
15. L. Nugent-Glandorf, T. A. Johnson, Y. Kobayashi, and S. A. Diddams, *Opt. Lett.* **36**, 1578 (2011).
16. F. Adler, K. C. Cossel, M. J. Thorpe, I. Hartl, M. E. Fermann, and J. Ye, *Opt. Lett.* **34**, 1330 (2009).
17. M. Charbonneau-Lefort, B. Afeyan, and M. M. Fejer, *J. Opt. Soc. Am. B* **25**, 463 (2008).
18. C. Heese, C. R. Phillips, L. Gallmann, M. M. Fejer, and U. Keller, *Opt. Express* **20**, 18066 (2012).